Inorganic Chemistry

Article

pubs.acs.org/IC

New Selenites: Hydrothermal Syntheses, Crystal Structures, and Characterization of $Rb_3HGa_2(OH)_2(SeO_3)_4$, $Rb_3Ga_5(SeO_3)_8(HSeO_3)_2{\cdot}0.5H_2O$, and $RbGa(SeO_3)_2{\cdot}H_2O$

Dong Woo Lee and Kang Min Ok*

Department of Chemistry, Chung-Ang University, 221 Heukseok-dong, Dongjak-gu, Seoul 156-756, Republic of Korea

Supporting Information

ABSTRACT: Three new gallium selenites, $Rb_3HGa_2(OH)_2(SeO_3)_4$, $Rb_3Ga_5(SeO_3)_8(HSeO_3)_2{\cdot}0.5H_2O$, and $RbGa(SeO_3)_2{\cdot}H_2O$, have been synthesized by hydrothermal reactions using Rb_2CO_3, $Ga(NO_3)_3{\cdot}xH_2O$, and SeO_2 as reagents. $Rb_3HGa_2(OH)_2(SeO_3)_4$ consists of unidimensional corner-linked chains of $GaO_4(OH)_2$ that are connected by a SeO_3 group, whereas $Rb_3Ga_5(SeO_3)_8(HSeO_3)_2{\cdot}0.5H_2O$ and $RbGa(SeO_3)_2{\cdot}H_2O$ exhibit three-dimensional frameworks consisting of three, mutually perpendicular, eight-membered rings (8-MRs). In all three reported materials, Se^{4+} is in an asymmetric coordination environment attributable to the stereoactive lone pair. Ion-exchange reactions, infrared spectroscopy, thermal analysis, elemental analysis, and dipole moment calculations for the reported materials are also presented. Crystal data: $Rb_3HGa_2(OH)_2(SeO_3)_4$, orthorhombic, space group *Cmca* (No. 64), with a = 7.17890(10) Å, b = 18.0925(2) Å, c = 12.6972(2) Å, and Z = 4; $Rb_3Ga_5(SeO_3)_8(HSeO_3)_2{\cdot}0.5H_2O$, triclinic, space group $P\bar{1}$ (No. 2), with a = 10.7727(2) Å, b = 12.5372(3) Å, c = 12.6952(3) Å, α = 87.210(10)°, β = 85.447(10)°, γ = 72.519(10)°, and Z = 2; $RbGaSe_2O_6{\cdot}H_2O$, triclinic, space group $P\bar{1}$ (No. 2), with a = 8.7027(6) Å, b = 9.7622(7) Å, c = 15.3347(14) Å, α = 105.622(4)°, β = 90.210(4)°, γ = 116.385(2)°, and Z = 2.

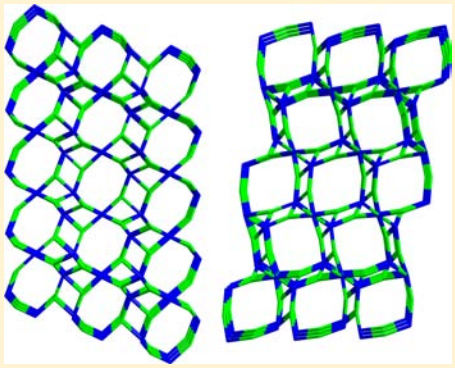

INTRODUCTION

Selenites, i.e., oxide materials containing Se^{4+} cation, have been of particular interest attributable to their rich structural chemistry.[1] The observed flexible structural backbones for selenite materials certainly come from the asymmetric coordination environment attributed to their stereoactive lone pairs. When the lone pair cations are combined with polyhedra of other metal cations and/or anions, a great deal of framework architectures and variable dimensions would be expected.[2] The dimensions of solid-state selenite materials with extended structures vary from low-dimensional molecular structures to three-dimensional frameworks. Among them, three-dimensional open-framework metal selenites with interesting structural architecture containing channels or pores have been of great interest attributed to their application in ion-exchange, catalysis, sorption, and storage.[3] In addition, selenite materials with asymmetric lone pair cations often crystallize in a space group with no center of symmetry and demonstrate technologically important properties such as second-harmonic-generating (SHG) properties.[4] The lone pairs are thought to be the result of a second-order Jahn−Teller (SOJT) distortions.[5] Synthetically, selenium dioxide (SeO_2) has been widely used as a reagent in the preparation of a variety of selenite materials due to its low triple point of 340 °C. The accessible temperature along with excellent reactivity and solubility of SeO_2 enabled it to be employed in the syntheses of many mixed-metal selenites materials. Although open-framework materials' chemistry has been extended, porous selenites materials are still relatively rare. We focused on discovering new selenites with richer structural chemistry by combining p elements. Recently, we reported a new family of quaternary metal selenites, $AM(SeO_3)_2$ (A = Li, Na, K, Rb, or Cs; M = Ga or In) and demonstrated that the size of alkali-metal cations influenced the framework structures as well as macroscopic centricities.[6] We further investigated the gallium selenite system to discover new selenites materials with asymmetric coordination environments. With respect to gallium(III) selenium(IV) oxides, several materials with various structural dimensions such as chains,[7] layers,[7,8] and three-dimensional frameworks[6b,7,8b,c,9] have been reported. Among them, while $[H_2en][GaF_3(SeO_3)]$[7] and $LiGa(SeO_3)_2$[6b] crystallize in noncentrosymmetric (NCS) space groups $CsGa_2H(SeO_3)_4{\cdot}2H_2O$[9a] and $Ga_2Se_2O_7$[8c] reveal open-framework structures. In this paper, we present the hydrothermal syntheses, crystal structures, and characterization of three new rubidium gallium selenites $Rb_3HGa_2(OH)_2(SeO_3)_4$, $Rb_3Ga_5(SeO_3)_8(HSeO_3)_2{\cdot}0.5H_2O$, and $RbGa(SeO_3)_2{\cdot}H_2O$. Ion-exchange behaviors and reversible hydration characteristics are also reported for the open-framework selenite, $RbGa(SeO_3)_2{\cdot}H_2O$.

EXPERIMENTAL SECTION

Syntheses. Rb_2CO_3 (Acros, 99.0%), $Ga(NO_3)_3{\cdot}xH_2O$ (Alfa Aesar, 99.9%), and SeO_2 (Aldrich, 98%) were used as received. For $Rb_3HGa_2(OH)_2(SeO_3)_4$, 0.693 g (3.00×10^{-3} mol) of Rb_2CO_3, 0.128 g (5.00×10^{-4} mol) of $Ga(NO_3)_3{\cdot}xH_2O$, 0.444 g (4.00×10^{-3} mol) of SeO_2,

Received: June 1, 2013
Published: August 16, 2013

   dx.doi.org/10.1021/ic4013894 | Inorg. Chem. 2013, 52, 10080−10086

Table 1. Crystallographic Data for $Rb_3HGa_2(OH)_2(SeO_3)_4$, $Rb_3Ga_5(SeO_3)_8(HSeO_3)_2{\cdot}0.5H_2O$, and $RbGa(SeO_3)_2{\cdot}H_2O$

formula	$Rb_3HGa_2Se_4O_{12}(OH)_2$	$Rb_3Ga_5Se_{10}O_{28}(OH)_2{\cdot}0.5H_2O$	$Rb_3Ga_3Se_6O_{18}{\cdot}2.4H_2O$
fw	938.71	1885.62	1270.56
space group	*Cmca* (No. 64)	*P*-1 (No. 2)	*P*-1 (No. 2)
a (Å)	7.17890(10)	10.7727(2)	8.7027(6)
b (Å)	18.0925(2)	12.5372(3)	9.7622(7)
c (Å)	12.6972(2)	12.6952(3)	15.3347(14)
α (deg)	90	87.210(10)	105.622(4)
β (deg)	90	85.447(10)	90.210(4)
γ (deg)	90	72.519(10)	116.385(2)
V (Å^3)	1649.17(4)	1629.70(6)	1112.42(15)
Z	4	2	2
T (°C)	298.0(2)	298.0(2)	298.0(2)
λ (Å)	0.71073	0.71073	0.71073
ρ_{calcd} (g cm^{-3})	3.781	3.836	3.779
μ (mm^{-1})	20.955	19.806	20.007
$R(F)^a$	0.0310	0.0423	0.0380
$R_w(F_o^2)^b$	0.0839	0.1093	0.0731

$^aR(F) = \Sigma||F_o| - |F_c||/\Sigma|F_o|$. $^bR_w(F_o^2) = [\Sigma w(F_o^2 - F_c^2)^2/\Sigma w(F_o^2)^2]^{1/2}$.

and 1 mL of deionized water were combined. For $Rb_3Ga_5(SeO_3)_8(HSeO_3)_2{\cdot}0.5H_2O$, 0.462 g ($2.00 \times 10^{-3}$ mol) of Rb_2CO_3, 0.256 g (1.00×10^{-3} mol) of $Ga(NO_3)_3{\cdot}xH_2O$, 0.444 g (4.00×10^{-3} mol) of SeO_2, and 0.5 mL of deionized water were combined. For $RbGaSe_2O_6{\cdot}H_2O$, 0.693 g (3.00×10^{-3} mol) of Rb_2CO_3, 0.384 g (1.50×10^{-3} mol) of $Ga(NO_3)_3{\cdot}xH_2O$, 0.444 g (4.00×10^{-3} mol) of SeO_2, and 2 mL of deionized water were combined. The respective reaction mixtures were placed in 23 mL Teflon-lined stainless steel autoclaves. The autoclaves were subsequently sealed and heated to 230 °C, held for 4 days, and cooled at a rate of 6 °C h^{-1} to room temperature. After cooling, the autoclaves were opened and products were recovered by filtration and washed with distilled water. Colorless crystals of $Rb_3HGa_2(OH)_2(SeO_3)_4$, $Rb_3Ga_5(SeO_3)_8(HSeO_3)_2{\cdot}0.5H_2O$, and $RbGa(SeO_3)_2{\cdot}H_2O$ were obtained in 33%, 38%, and 40% yields, respectively, based on rubidium carbonate. The final pH values were 3, 4, and 8 for $Rb_3HGa_2(OH)_2(SeO_3)_4$, $Rb_3Ga_5(SeO_3)_8(HSeO_3)_2{\cdot}0.5H_2O$, and $RbGa(SeO_3)_2{\cdot}H_2O$, respectively.

Single-Crystal X-ray Diffraction. The structures of the reported materials were determined by a standard crystallographic method. A colorless rod ($0.015 \times 0.021 \times 0.056$ mm^3) for $Rb_3HGa_2(OH)_2(SeO_3)_4$, a colorless block ($0.035 \times 0.042 \times 0.071$ mm^3) for $Rb_3Ga_5(SeO_3)_8(HSeO_3)_2{\cdot}0.5H_2O$, and a colorless block ($0.022 \times 0.034 \times 0.042$ mm^3) for $RbGa(SeO_3)_2{\cdot}H_2O$ were used for single-crystal data analyses. All data were collected using a Bruker SMART BREEZE diffractometer equipped with a 1K CCD area detector using graphite-monochromated Mo Kα radiation at room temperature. A hemisphere of data was collected using a narrow-frame method with scan widths of 0.30° in omega and an exposure time of 10 s/frame. The first 50 frames were remeasured at the end of the data collection to monitor instrument and crystal stability. The maximum correction applied to the intensities was <1%. Data were integrated using the SAINT program,[10] with the intensities corrected for Lorentz factor, polarization, air absorption, and absorption attributable to the variation in the path length through the detector faceplate. A semiempirical absorption correction was made on the hemisphere of data with the SADABS program.[11] Data were solved and refined using SHELXS-97[12] and SHELXL-97,[13] respectively. All calculations were performed using the WinGX-98 crystallographic software package.[14] Crystallographic data for the reported materials are given in Table 1.

Powder X-ray Diffraction. Powder X-ray diffraction was used to confirm the phase purity of the synthesized materials. Powder XRD patterns were collected on a Bruker D8-Advance diffractometer using Cu Kα radiation at room temperature with 40 kV and 40 mA. Polycrystalline samples were mounted on sample holders and scanned in the 2θ range 5−70° with a step size of 0.02° and step time of 0.2 s.

Infrared Spectroscopy. Infrared spectra were recorded on a Varian 1000 FT-IR spectrometer in the 400−4000 cm^{-1} range with the sample embedded in a KBr matrix.

Thermogravimetric Analysis. Thermogravimetric analyses were performed on a Setaram LABSYS TG-DTA/DSC Thermogravimetric Analyzer. Polycrystalline samples were contained within alumina crucibles and heated at a rate of 10 °C min^{-1} from room temperature to 1000 °C under flowing argon.

Scanning Electron Microscope/Energy-Dispersive Analysis by X-ray (SEM/EDAX). SEM/EDAX analysis has been performed using a Hitachi S-3400N/Horiba Energy EX-250 instruments. EDAX for $Rb_3HGa_2(OH)_2(SeO_3)_4$, $Rb_3Ga_5(SeO_3)_8(HSeO_3)_2{\cdot}0.5H_2O$, and $RbGa(SeO_3)_2{\cdot}H_2O$ exhibit Rb/Ga/Se ratios of approximately 1.4:1.0:2.1, 1.0:1.7:3.4, and 1.0:1.0:1.8, respectively.

Ion-Exchange Experiments. Ion-exchange reactions were performed by stirring ca. 100 mg of polycrystalline $RbGa(SeO_3)_2{\cdot}H_2O$ in 5 mL of 0.1 M HCl (aq) and 1 M KNO_3 (aq) solutions. Reactions were performed at room temperature for 24 h and then at 80 °C for 72 h. The ion-exchanged products were recovered by filtration, washed with excess water, and dried in air for 1 day.

RESULTS AND DISCUSSION

Structures. *$Rb_3HGa_2(OH)_2(SeO_3)_4$.* $Rb_3HGa_2(OH)_2(SeO_3)_4$ has a unidimensional crystal structure composed of parallel chains of corner-shared $GaO_4(OH)_2$ octahedra. Each $GaO_4(OH)_2$ octahedron shares additional corners with the SeO_3 group (see Figure 1a). The Se^{4+} cations are in asymmetric coordination environment attributable to their stereoactive lone pairs. The lone pairs on the Se^{4+} point approximately toward the [001] and [00−1] directions. The chains run parallel to the *a* axis and are separated by the Rb^+ cations (see Figure 1b). The observed Ga^{3+}−O bond distances range from 1.9605(18) to 2.023(3) Å and the O−Ga^{3+}−O bond angles range from 86.39(16)° to 177.52(13)°. The Se^{4+}−O bond lengths and O−Se^{4+}−O bond angles range 1.653(5)−1.707(5) Å and 100.70(17)−101.1(2)°, respectively. The two unique $Rb^+(1)$ and $Rb^+(2)$ cations contact with nine and six oxygen atoms, respectively, with Rb−O contact distances in the range 2.746(5)−3.382(3) Å. Bond-valence sum (BVS) calculations[15] were used to identify the positions of the hydrogen atom. BVS calculations on oxygen atoms reveal values of 2.164, 1.074, 1.986, 1.549, and 1.882 for O(1), O(2), O(3), O(4), and O(5), respectively, which strongly indicates H^+ is bonded to O(2). The IR spectrum for $Rb_3HGa_2(OH)_2(SeO_3)_4$ confirms the presence of the coordinated OH group. Similar chain structure of gallium oxide polyhedra with OH group has been observed before.[16] In connectivity terms, the structure of $Rb_3HGa_2(OH)_2(SeO_3)_4$ can be formulated as anionic chains of

dx.doi.org/10.1021/ic4013894 | Inorg. Chem. 2013, 52, 10080−10086

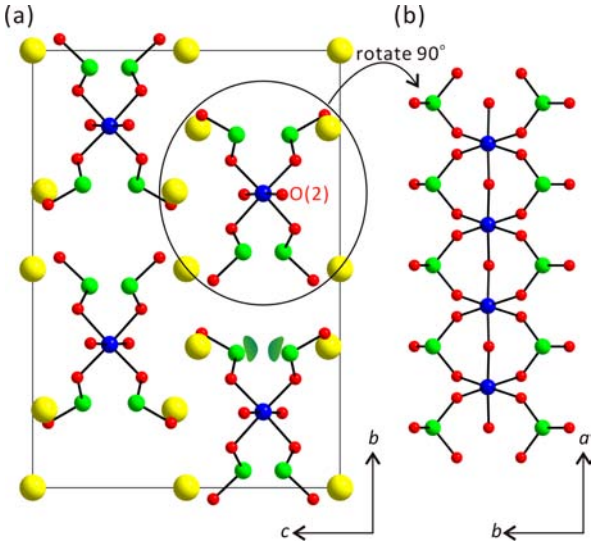

Figure 1. Ball-and stick model of $Rb_3HGa_2(OH)_2(SeO_3)_4$ in the (a) *bc* and (b) *ab* planes (green, Se^{4+}; blue, Ga^{3+}; yellow, Rb^+; red, O). Note the chains consisting of corner-shared $GaO_4(OH)_2$ octahedra and SeO_3 groups are running along the *a* axis.

$\{[Ga^{3+}O_{4/2}(OH)_{2/2}]^{-2}\ 2[Se^{4+}O_{2/2}O_{1/1}]^0\}^{-2}$, with charge balance retained by the Rb^+ and H^+ cations. Bond-valence calculations[15] for the Rb^+, Ga^{3+}, and Se^{4+} result in values in ranges of 0.74−1.18, 3.05, and 4.09−4.20, respectively.

$Rb_3Ga_5(SeO_3)_8(HSeO_3)_2{\cdot}0.5H_2O$. $Rb_3Ga_5(SeO_3)_8(HSeO_3)_2{\cdot}0.5H_2O$ has a three-dimensional structure consisting of SeO_3 polyhedra connected to GaO_4 tetrahedra and GaO_6 octahedra through the oxygen atoms (see Figure 2). Within an asymmetric unit, five unique Ga^{3+} cations exist. While $Ga(1)^{3+}$ is bonded to four oxygen atoms, the other four Ga^{3+} cations are connected to six oxygen atoms. The Ga−O bond distances in GaO_4 tetrahedra range from 1.833(5) to 1.846(5) Å, whereas those in GaO_6 octahedra range from 1.932(5) to 2.016(5) Å. The O−Ga−O bond angles for GaO_4 tetrahedra and GaO_6 octahedra range 96.4(2)−118.7(2)° and 83.2(2)−178.0(2)°, respectively. The ten Se^{4+} cations are all linked to three oxygen atoms and exhibit three-coordinate asymmetric SeO_3 polyhedra. Se−O bond lengths range from 1.644(5) to 1.759(5) Å and the O−Se−O bond angles range from 93.1(2)° to 105.6(2)°. The three unique Rb^+ cations, $Rb(1)^+$, $Rb(2)^+$, and $Rb(3)^+$, contact with 11, 12, and 8 oxygen atoms, respectively, with Rb−O contact distances in the range 2.810(5)−3.583(5) Å. Similar to $Rb_3HGa_2(OH)_2(SeO_3)_4$, we found that two oxygen atoms should be −OH groups. Bond-valence sum calculations[15] on the oxygen sites resulted in values ranging from 1.82 to 2.18 for most oxygen atoms. However, BVS calculations for O(24) and O(30) show values of 1.15 and 1.28, respectively, which strongly indicates the hydrogen atoms must be attached to the two oxygen atoms. The result is consistent with the Se−O bond lengths: while the Se(8)−O(24) and Se(10)−O(30) bonds exhibit the longest distances of 1.755(8) and 1.759(5) Å, the other Se−O bonds reveal shorter distances ranging from 1.644(5) to 1.737(5) Å. Similar Se−O distance ranges have been observed from previously reported materials containing a hydrogen selenite group.[1b,f,8a] Finally, the infrared spectrum of $Rb_3Ga_5(SeO_3)_8(HSeO_3)_2{\cdot}0.5H_2O$ supports the presence of the Se−O−H groups in the material (see Infrared Spectroscopy).

As can be seen in Figures 2−4, $Rb_3Ga_5(SeO_3)_8(HSeO_3)_2{\cdot}0.5H_2O$ has a three-dimensional framework structure consisting

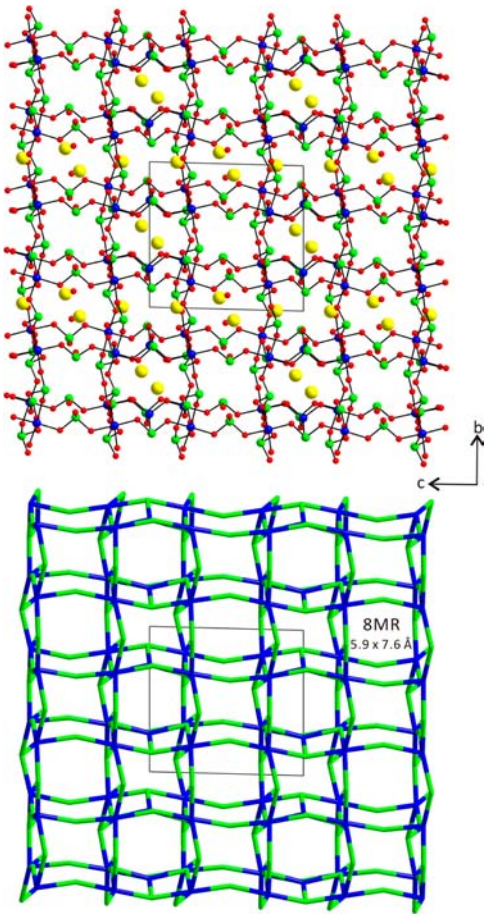

Figure 2. Ball-and-stick and wire representation of $Rb_3Ga_5(SeO_3)_8(HSeO_3)_2{\cdot}0.5H_2O$ showing the 8-MR channels along the [100] direction (green, Se^{4+}; blue, Ga^{3+}; yellow, Rb^+; red, O).

of three, mutually perpendicular, eight-membered rings (8-MR) along the [100], [010], and [001] directions. Each channel is composed of four GaO_6 octahedra and four SeO_3 polyhedra that alternate around the ring. The framework of $Rb_3Ga_5(SeO_3)_8(HSeO_3)_2{\cdot}0.5H_2O$ can be also described as a combination of two kinds of distorted cubes. Eight GaO_6 octahedra and eight SeO_3 polyhedra share their corners through oxygen atoms and form a distorted cube (see Figure 4). In other words, each GaO_6 octahedron is located in the corners and SeO_3 groups serve as linkers to complete a distorted simple cubic building block. Another kind of distorted cubic building block is observed: four SeO_3 polyhedra in each parallel face of the distorted cube further share their corners with a GaO_4 tetrahedron, which results in a distorted end-centered cubic structure. The distorted end-centered cubic structure, however, impedes movement of the Rb^+ cations along the [010] direction. In connectivity terms, the structure can be represented as consisting of an anionic framework of $\{4[GaO_{6/2}]^{3-}\ [GaO_{4/2}]^-\ 8[SeO_{3/2}]^+\ 2[SeO_{2/2}(OH)]^+\}^{3-}$. Charge neutrality is maintained by the Rb^+ cations. Bond-valence calculations on $Rb_3Ga_5(SeO_3)_8(HSeO_3)_2{\cdot}0.5H_2O$ reveal values ranging from 4.04 to 4.23 for Se^{4+} and 2.97 to 3.22 for Ga^{3+}.[15] The 8-MRs are similar in size, taking into account the atomic radii of oxygen,[17] with dimensions of 5.9 Å × 7.6 Å [100], 5.3 × 5.3 Å [010], and 5.0 × 5.5 Å [001]. Rb^+ cations and occluded water molecules are within the rings.

Since $Rb_3Ga_5(SeO_3)_8(HSeO_3)_2{\cdot}0.5H_2O$ exhibits a moderately open-framework structure, the amount of void space has been

dx.doi.org/10.1021/ic4013894 | *Inorg. Chem.* 2013, 52, 10080−10086

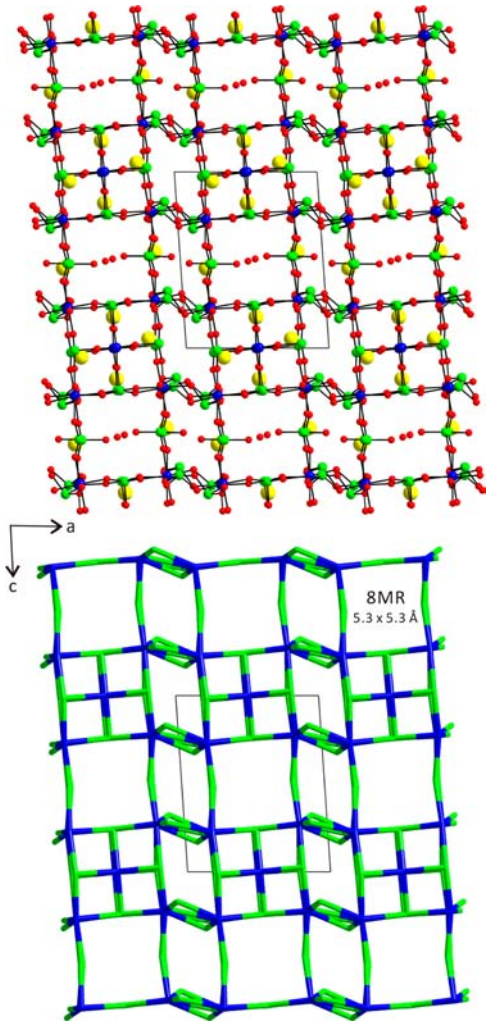

Figure 3. Ball-and-stick and wire representation of $Rb_3Ga_5(SeO_3)_8(HSeO_3)_2{\cdot}0.5H_2O$ showing the 8-MR channels along the [010] direction (green, Se^{4+}; blue, Ga^{3+}; yellow, Rb^+; red, O).

molecules are included in the calculation, the void space for $Rb_3Ga_5(SeO_3)_8(HSeO_3)_2{\cdot}0.5H_2O$ becomes 2.4%.

$RbGaSe_2O_6{\cdot}H_2O$. $RbGa(SeO_3)_2{\cdot}H_2O$ exhibits another three-dimensional framework structure consisting of SeO_3 polyhedra connected to GaO_6 octahedra through the oxygen atoms (see Figure 5). In connectivity terms, the structure may be described

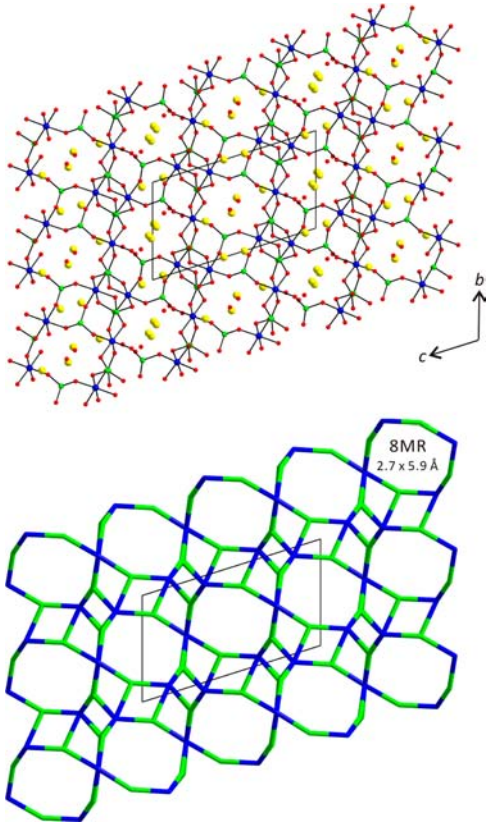

Figure 5. Ball-and-stick and wire representation of $RbGa(SeO_3)_2{\cdot}H_2O$ exhibiting the 8-MR channels along the [100] direction (green, Se^{4+}; blue, Ga^{3+}; yellow, Rb^+; red, O).

calculated by removing all of the nonframework species, Rb^+, and occluded water molecules and using the CALC SOLV command in PLATON.[18] For $Rb_3Ga_5(SeO_3)_8(HSeO_3)_2{\cdot}0.5H_2O$, the amount of void space is 15.3%. Once the Rb^+ and water

as an anionic framework of $\{6[SeO_{3/2}]^+3[GaO_{6/2}]^{3-}\}^{3-}$. Charge balance is maintained by the incorporation of the Rb^+ cations. The Rb^+ cations are disordered over six different positions with partial occupancies. Fractional occupancies of 0.598(3),

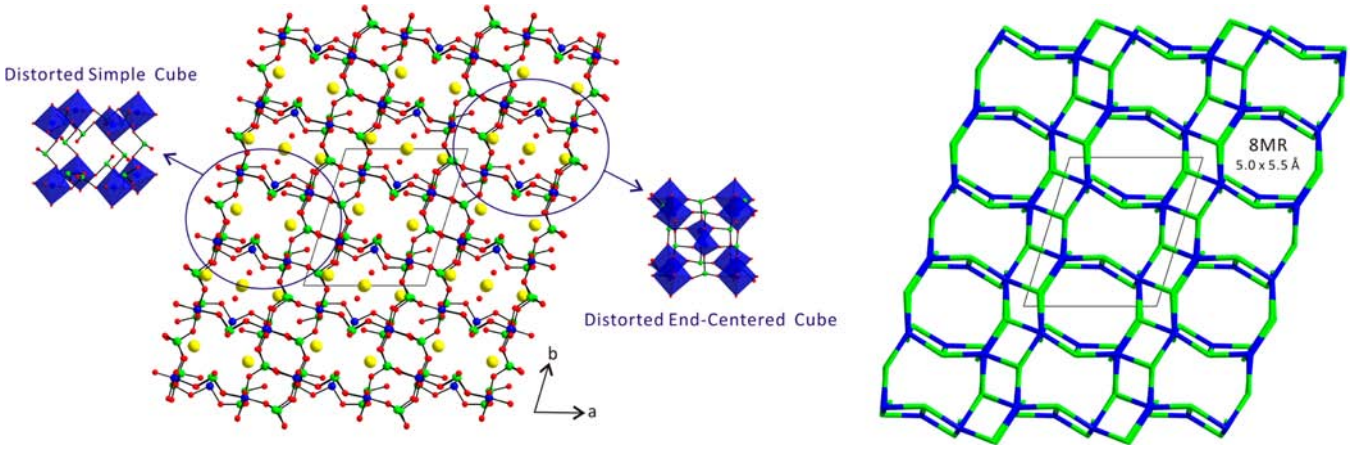

Figure 4. Ball-and-stick and wire representation of $Rb_3Ga_5(SeO_3)_8(HSeO_3)_2{\cdot}0.5H_2O$ showing the 8-MR channels along the [001] direction (green, Se^{4+}; blue, Ga^{3+}; yellow, Rb^+; red, O).

dx.doi.org/10.1021/ic4013894 | *Inorg. Chem.* 2013, 52, 10080−10086

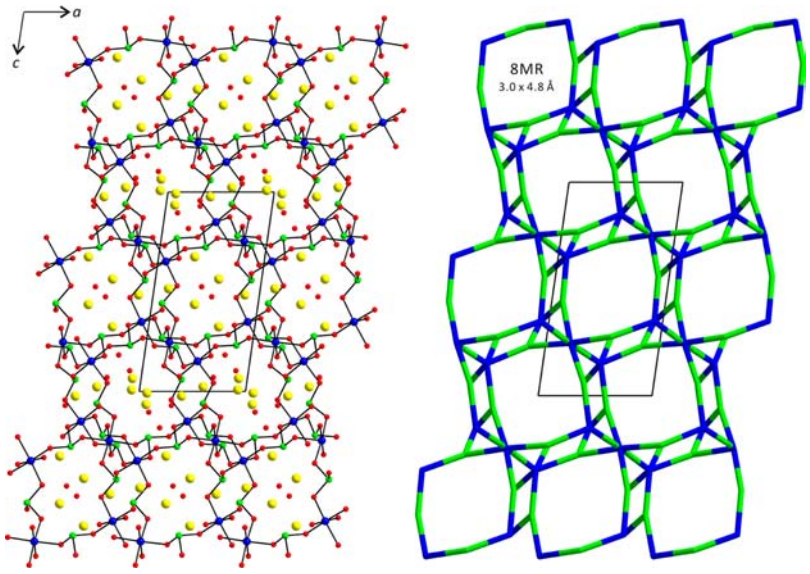

Figure 6. Ball-and-stick and wire representation of $RbGa(SeO_3)_2{\cdot}H_2O$ exhibiting the 8-MR channels along the [010] direction (green, Se^{4+}; blue, Ga^{3+}; yellow, Rb^+; red, O).

0.488(3), 0.578(3), 0.611(3), 0.423(3), and 0.290(3) were refined for Rb(1), Rb(2), Rb(3), Rb(4), Rb(5), and Rb(6), respectively, which successfully retains charge balance of the material. Bond-valence sum calculations[15] resulted in values ranging from 3.98 to 4.08 for Se^{4+} and 3.02 to 3.03 for Ga^{3+}. The observed Ga−O bond distances and the O−Ga−O bond angles range 1.960(4)−2.013(4) Å and 83.47(17)−179.82(18)°, respectively. The six unique Se^{4+} cations are linked to three oxygen atoms and form SeO_3 polyhedra with Se−O bond lengths and O−Se−O bond angles ranging 1.686(4)−1.715(4) Å and 97.5(2)−101.1(2)°, respectively.

Similar to that of $Rb_3Ga_5(SeO_3)_8(HSeO_3)_2{\cdot}0.5H_2O$, the structural backbone of $RbGa(SeO_3)_2{\cdot}H_2O$ can be considered as a framework composed of three, mutually perpendicular, eight-membered ring (8-MR) channels running along the [100], [010], and [001] directions (see Figures 5−7). The dimensions of the channels are 3.0 × 5.9 Å [100], 3.0 × 4.8 Å [010], and 3.0 × 3.2 Å [001] taking into account the atomic radii of oxygen.[17] The dimension for the 8-MR perpendicular to the [001] direction is relatively small, since the 8-MRs along the *c* direction are interwoven and the backbone is overlapped (see Figure 7). The amount of void space for $RbGa(SeO_3)_2{\cdot}H_2O$ can be also calculated after excluding Rb^+ cations and water molecules using the CALC SOLV command in the PLATON crystallographic tool.[18] The calculated void space for $RbGa(SeO_3)_2{\cdot}H_2O$ is about 36%, which is smaller than the analogous values for cloverite (60%) and faujasite (84%). However, when the nonframework elements, the disordered Rb^+ cations, and the water molecules are included in the calculation, the void space for $RbGa(SeO_3)_2{\cdot}H_2O$ becomes zero.

Infrared Spectroscopy. The infrared spectra of $Rb_3HGa_2(OH)_2(SeO_3)_4$, $Rb_3Ga_5(SeO_3)_8(HSeO_3)_2{\cdot}0.5H_2O$, and $RbGa(SeO_3)_2{\cdot}H_2O$ reveal Ga−O and Se−O stretching vibrations between ca. 418 and 480 and ca. 509 and 814 cm^{-1}. The bands occurring at 865 and 3400 cm^{-1} for $Rb_3HGa_2(OH)_2(SeO_3)_4$ are attributable to the Ga−O−H vibrations, while a characteristic band at 1195 cm^{-1} for $Rb_3Ga_5(SeO_3)_8(HSeO_3)_2{\cdot}0.5H_2O$ is ascribed to the Se−O−H bond in the hydrogen selenite group. Finally, for $Rb_3Ga_5(SeO_3)_8(HSeO_3)_2{\cdot}0.5H_2O$ and $RbGaSe_2O_6{\cdot}H_2O$ vibrations attributable to H_2O are observed at 1615−1654 and 3420−3493 cm^{-1}. IR spectra for the reported materials have been also deposited in the Supporting Information. Assignments are consistent with those previously reported.[9c,19]

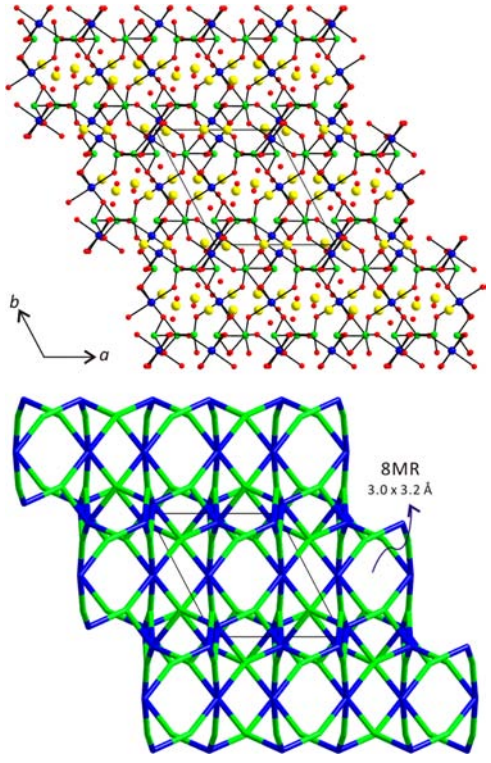

Figure 7. Ball-and-stick and wire representation of $RbGa(SeO_3)_2{\cdot}H_2O$ exhibiting the 8-MR channels along the [001] direction (green, Se^{4+}; blue, Ga^{3+}; yellow, Rb^+; red, O).

Thermal Analysis. Thermogravimetric analysis (TGA) has been used to investigate the thermal behavior of the reported materials. $Rb_3HGa_2(OH)_2(SeO_3)_4$ is stable up to 210 °C. Above 210 °C, loss of a H_2O molecule is observed with a total weight loss of 2.61% (calcd 1.92%). The dehydrated material shows crystallinity with similar framework structure to that of $Rb_3HGa_2(OH)_2(SeO_3)_4$ based on the PXRD patterns up to

dx.doi.org/10.1021/ic4013894 | *Inorg. Chem.* 2013, 52, 10080−10086

320 °C (see the Supporting Information). Above the temperature, the material starts decomposing attributable to sublimation of SeO_2. $Rb_3Ga_5(SeO_3)_8(HSeO_3)_2{\cdot}0.5H_2O$ exhibits a weight loss of 0.30% between room temperature and 260 °C that is attributed to loss of the occluded water molecules (calcd 0.48%). The PXRD pattern measured for the sample heated to 400 °C is very similar to the mixture of $CsGaSe_2O_6$[6b] and $Ga_2Te_4O_{11}$,[20] which strongly suggests that the material loses H_2O and O_2 up to 400 °C and changes to $RbGaSe_2O_6$ and $Ga_2Se_4O_{11}$. Then the material completely decomposes due to loss of SeO_2. $RbGa(SeO_3)_2{\cdot}H_2O$ reveals an initial weight loss of 4.85% between room temperature and 300 °C, which is attributable to loss of 1 equiv of occluded water (calcd 4.22%). The dehydrated material is thermally stable up to 360 °C. Interestingly, loss of occluded water molecules from $RbGa(SeO_3)_2{\cdot}H_2O$ is fully reversible once the material is heated to 300 °C then cooled back to room temperature. Complete rehydration occurs when the activated material was exposed to water vapor for 15 min, which was confirmed by PXRD (see the Supporting Information). Above 360 °C, decomposition attributable to elimination of SeO_2 occurs. The TGA plots for all three materials and PXRD data obtained at different temperatures are shown in the Supporting Information.

Ion-Exchange Experiments. The open-framework structure of $RbGa(SeO_3)_2{\cdot}H_2O$ suggested the material might be subjected to ion-exchange reactions, where the Rb^+ could be replaced by other cations. We were able to completely exchange the Rb^+ cation for H^+ and K^+ by stirring a suspension of the host material in 0.1 and 1 M solutions of HCl and KNO_3, respectively, for 1 day at room temperature and then an additional 3 days at 80 °C. Elemental analyses reveal no Rb^+ cation is observed at all from the ion-exchanged products. Powder X-ray diffraction data show similar diffraction patterns and highly crystalline materials for both the H^+- and K^+-exchanged products (see the Supporting Information). In addition, the ion-exchanged materials may be indexed on rhombohedral cells with $a = b = 8.419(2)$ Å, $c = 24.530(9)$ Å, and $V = 1505.6(7)$ Å^3 for H^+-exchanged product and $a = b = 9.272(2)$ Å, $c = 26.095(6)$ Å, and $V = 1942.7(6)$ Å^3 for K^+-exchanged compound. However, ion-exchange attempts on another open-framework $Rb_3Ga_5(SeO_3)_8(HSeO_3)_2{\cdot}0.5H_2O$ under similar conditions indicated that exchanging Rb^+ for other cations was difficult. It seems that the distorted end-centered cubic lattices impede movement of the Rb^+ cations and lock up the channel windows in $Rb_3Ga_5(SeO_3)_8(HSeO_3)_2{\cdot}0.5H_2O$.

Dipole Moment Calculations. Since all three reported materials contain a cation (Se^{4+}) exhibiting an asymmetric coordination environment, we thought that it would be better to calculate the local dipole moments for Se^{4+} cations to better understand the asymmetric coordination environment. Specifically, the direction and magnitude of the distortions in the SeO_3 group can be quantified by determining the local dipole moments. This method has been described before with respect to octahedra of metal oxy−fluoride using a bond-valence approach.[21] For the polyhedra for lone pair cations, the lone pair is assigned a charge of −2 and the localized Se^{4+}−lone pair distance is estimated to be 1.22 Å on the basis of previous work by Galy and Meunier.[22] Using this methodology, we found that the local dipole moments for the SeO_3 polyhedra in the reported materials are in the range of 7.35−8.51 D (where D denotes Debyes), with an average value of 7.93 D (see the Supporting Information). The values are consistent with those reported dipole moments for SeO_3 polyhedra.[1g−i,6,23]

CONCLUSIONS

Three new mixed-metal selenites, $Rb_3HGa_2(OH)_2(SeO_3)_4$, $Rb_3Ga_5(SeO_3)_8(HSeO_3)_2{\cdot}0.5H_2O$, and $RbGa(SeO_3)_2{\cdot}H_2O$, have been successfully synthesized by hydrothermal reactions. The materials were structurally characterized by X-ray diffraction. While $Rb_3HGa_2(OH)_2(SeO_3)_4$ exhibits a unidimensional structure consisting of corner-shared $GaO_4(OH)_2$ octahedra, $Rb_3Ga_5(SeO_3)_8(HSeO_3)_2{\cdot}0.5H_2O$ and $RbGa(SeO_3)_2{\cdot}H_2O$ reveal three-dimensional frameworks composed of three, mutually perpendicular, 8-MR channels along the [100], [010], and [001] directions. The open-framework material $RbGa(SeO_3)_2{\cdot}H_2O$ shows a robust ion-exchange behavior as well as reversible dehydration/rehydration properties.

ASSOCIATED CONTENT

Supporting Information

X-ray crystallographic file in CIF format, calculated and observed X-ray diffraction patterns, infrared spectra, thermal analysis diagrams, and powder X-ray diffraction patterns of ion-exchanged products for $Rb_3HGa_2(OH)_2(SeO_3)_4$, $Rb_3Ga_5(SeO_3)_8(HSeO_3)_2{\cdot}0.5H_2O$, and $RbGaSe_2O_6{\cdot}H_2O$. This material is available free of charge via the Internet at http://pubs.acs.org.

AUTHOR INFORMATION

Corresponding Author

*Phone: +82-2-820-5197 Fax: +82-2-825-4736. E-mail: kmok@cau.ac.kr.

Notes

The authors declare no competing financial interest.

ACKNOWLEDGMENTS

This research was supported by the Basic Science Research Program through the National Research Foundation of Korea (NRF) funded by the Ministry of Education, Science & Technology (grant 2013R1A2A2A01007170).

REFERENCES

(1) (a) Morris, R.; Harrison, W. T. A.; Stucky, G. D.; Cheetham, A. K. *Acta Crystallogr., Sect. C* **1992**, *48*, 1182. (b) Castro, A.; Enjalbert, R.; Pedro, M. d.; Trombe, J. C. *J. Solid State Chem.* **1994**, *112*, 418. (c) Effenberger, H. *Acta Chem. Scand.* **1996**, *50*, 967. (d) Effenberger, H. *J. Alloys Compd.* **1998**, *281*, 152. (e) Rademacher, O.; Goebel, H.; Oppermann, H. *Z. Kristallogr. - New Cryst. Struct.* **2000**, *215*, 339. (f) Burns, W. L.; Ibers, J. A. *J. Solid State Chem.* **2009**, *182*, 1457. (g) Lee, D. W.; Ok, K. M. *Solid State Sci.* **2010**, *12*, 2036. (h) Oh, S.-J.; Lee, D. W.; Ok, K. M. *Inorg. Chem.* **2012**, *51*, 5393. (i) Oh, S.-J.; Lee, D. W.; Ok, K. M. *Dalton Trans.* **2012**, *41*, 2995.

(2) (a) Semenova, T. F.; Rozhdestvenskaya, I. V.; Filatov, S. K.; Vergasova, L. P. *Miner. Mag.* **1992**, *56*, 241. (b) Johnsson, M.; Tornroos, K. W.; Mila, F.; Millet, P. *Chem. Mater.* **2000**, *12*, 2853. (c) Millet, P.; Bastide, B.; Pashchenko, V.; Gnatchenko, S.; Gapon, V.; Ksari, Y.; Stepanov, A. *J. Mater. Chem.* **2001**, *11*, 1152. (d) Millet, P.; Johnsson, M.; Pashchenko, V.; Ksari, Y.; Stepanov, A.; Mila, F. *Solid State Ionics* **2001**, *141*, 559. (e) Becker, R.; Johnsson, M.; Kremer, R. K.; Lemmens, P. *Solid State Sci.* **2003**, *5*, 1411. (f) Mayerová, Z.; Johnsson, M.; Lidin, S. *J. Solid State Chem.* **2005**, *178*, 3471. (g) Mayerová, Z.; Johnsson, M.; Lidin, S. *Angew. Chem., Int. Ed.* **2006**, *45*, 5602. (h) Jo, V.; Kim, M. K.; Lee, D. W.; Shim, I.-W.; Ok, K. M. *Inorg. Chem.* **2010**, *49*, 2990. (i) Kim, M. K.; Jo, V.; Lee, D. W.; Ok, K. M. *Dalton Trans.* **2010**, *39*, 6037.

(3) (a) Choudhury, A.; Kumar D, U.; Rao, C. N. R. *Angew. Chem., Int. Ed.* **2002**, *41*, 158. (b) Pasha, I.; Choudhury, A.; Rao, C. N. R. *Solid State Sci.* **2003**, *5*, 257. (c) Pasha, I.; Choudhury, A.; Rao, C. N. R. *Inorg. Chem.* **2003**, *42*, 409. (d) Rao, C. N. R.; Dan, M.; Behera, J. N. *Pure Appl. Chem.* **2005**, *77*, 1655. (e) Rao, C. N. R.; Behera, J. N.; Dan, M. *Chem. Soc. Rev.*

2006, *35*, 375. (f) Xiao, D.; An, H.; Wang, E.; Sun, C.; Xu, L. *J. Coord. Chem.* **2006**, *59*, 395. (g) Natarajan, S.; Mandal, S. *Angew. Chem., Int. Ed.* **2008**, *47*, 4798.
(4) (a) *Principles and Applications of Ferroelectrics and Related Materials*; Lines, M. E., Glass, A. M., Eds.; Oxford University Press: Oxford, U.K., 1991. (b) Ok, K. M.; Chi, E. O.; Halasyamani, P. S. *Chem. Soc. Rev.* **2006**, *35*, 710.
(5) (a) Opik, U.; Pryce, M. H. L. *Proc. R. Soc. London* **1957**, *A238*, 425. (b) Bader, R. F. W. *Mol. Phys.* **1960**, *3*, 137. (c) Bader, R. F. W. *Can. J. Chem.* **1962**, *40*, 1164. (d) Pearson, R. G. *J. Mol. Struct.: THEOCHEM* **1983**, *103*, 25. (e) Wheeler, R. A.; Whangbo, M.-H.; Hughbanks, T.; Hoffmann, R.; Burdett, J. K.; Albright, T. A. *J. Am. Chem. Soc.* **1986**, *108*, 2222.
(6) (a) Lee, D. W.; Kim, S. B.; Ok, K. M. *Inorg. Chem.* **2012**, *51*, 8530. (b) Lee, D. W.; Ok, K. M. *Inorg. Chem.* **2013**, *52*, 5176.
(7) Feng, M.-L.; Li, X.-L.; Mao, J.-G. *Cryst. Growth Des.* **2007**, *7*, 770.
(8) (a) Morris, R. E.; Cheetham, A. K. *Chem. Mater.* **1994**, *6*, 67. (b) Kong, F. L.; Qi-Pu; Yi, F.-Y.; Mao, J.-G. *Inorg. Chem.* **2009**, *48*, 6794. (c) Kong, F.; Li, P.-X.; Zhang, S.-Y.; Mao, J.-G. *J. Solid State Chem.* **2012**, *190*, 118.
(9) (a) Rastsvetaeva, R. K.; Petrova, G. K.; Andrianov, V. I. *Dokl. Akad. Nauk SSSR* **1983**, *270*, 882. (b) Rastsvetaeva, R. K.; Andrianov, V. I.; Volodina, A. N. *Dokl. Akad. Nauk SSSR* **1986**, *291*, 352. (c) Ok, K. M.; Halasyamani, P. S. *Chem. Mater.* **2002**, *14*, 2360. (d) Kong, F.; Hu, C.-L.; Hu, T.; Zhou, Y.; Mao, J.-G. *Dalton Trans.* **2009**, *25*, 4962.
(10) *SAINT Program for Area Detector Absorption Correction*, version 4.05; Siemens Analytical X-ray Instruments: Madison, WI, 1995.
(11) Blessing, R. H. *Acta Crystallogr., Sect. A* **1995**, *51*, 33.
(12) Sheldrick, G. M. *SHELXS-97: A program for automatic solution of crystal structures*; University of Goettingen: Goettingen, Germany, 1997.
(13) Sheldrick, G. M. *SHELXL-97: A program for crystal structure refinement*; University of Goettingen: Goettingen, Germany, 1997.
(14) Farrugia, L. J. *J. Appl. Crystallogr.* **1999**, *32*, 837.
(15) (a) Brown, I. D.; Altermatt, D. *Acta Crystallogr., Sect. B* **1985**, *41*, 244. (b) Brese, N. E.; O'Keeffe, M. *Acta Crystallogr., Sect. B* **1991**, *47*, 192.
(16) Kim, M. K.; Jo, V.; Shim, I.-W.; Ok, K. M. *Inorg. Chem.* **209**, *48*, 1275.
(17) Shannon, R. D. *Acta Crystallogr.* **1976**, *A32*, 751.
(18) Spek, A. L. *Platon: A Multi-purpose Crystallographic Tool*; Utrecht University: Utrecht, The Netherlands, 2001.
(19) (a) Muilu, H.; Valkonen, J. *Acta Chem. Scand.* **1987**, *A41*, 183. (b) Kong, F.; Xu, X.; Mao, J. G. *Inorg. Chem.* **2010**, *49*, 11573. (c) Lee, D. W.; Bak, D.-b.; Kim, S. B.; Kim, J.; Ok, K. M. *Inorg. Chem.* **2012**, *51*, 7844.
(20) Dutreilh, M.; Thomas, P.; Champarnaud-Mesjard, J. C.; Frit, B. *Solid State Sci.* **2001**, *3*, 423.
(21) (a) Maggard, P. A.; Nault, T. S.; Stern, C. L.; Poeppelmeier, K. R. *J. Solid State Chem.* **2003**, *175*, 27. (b) Izumi, H. K.; Kirsch, J. E.; Stern, C. L.; Poeppelmeier, K. R. *Inorg. Chem.* **2005**, *44*, 884.
(22) Galy, J.; Meunier, G. *J. Solid State Chem.* **1975**, *13*, 142.
(23) (a) Ok, K. M.; Halasyamani, P. S. *Inorg. Chem.* **2005**, *44*, 3919. (b) Lee, D. W.; Oh, S.-J.; Halasyamani, P. S.; Ok, K. M. *Inorg. Chem.* **2011**, *50*, 4473. (c) Oh, S.-J.; Shin, Y.; Tran, T. T.; Lee, D. W.; Yoon, A.; Halasyamani, P. S.; Ok, K. M. *Inorg. Chem.* **2012**, *51*, 10402.